Electronic Supplementary Material (ESI) for Dalton Transactions.

Supplementary Information

Fluorescence and room temperature activity of Y_2O_3:(Eu^{3+},Au^{3+})/palygorskite nanocomposite

Xi He and Huaming Yang *

Table S1 Distances of planes in different samples.

Sample	Y_2O_3:Eu^{3+}	Au-1	Au-2	Au-3	Au-4	Au-5
$d_{(222)}$ / Å	3.0744 (0.0008)	3.0699 (0.0005)	3.0701 (0.0009)	3.0654 (0.0008)	3.0638 (0.0009)	3.0615 (0.0007)
$d_{(440)}$ / Å	1.8805 (0.0005)	1.8793 (0.0005)	1.8787 (0.0004)	1.8769 (0.0004)	1.8764 (0.0003)	1.8761 (0.0003)
$d_{(622)}$ / Å	1.6037 (0.0004)	1.6025 (0.0005)	1.6018 (0.0004)	1.6013 (0.0004)	1.6008 (0.0003)	1.6003 (0.0003)

Note: The errors were shown in the parentheses.

Table S2 FWHM values of Au doped samples

Sample	Au-1	Au-2	Au-3	Au-4	Au-5
$FWHM_{(222)}$ / °	0.284 (0.005)	0.268 (0.005)	0.260 (0.004)	0.290 (0.006)	0.385 (0.006)
$FWHM_{(440)}$ / °	0.285 (0.005)	0.271 (0.005)	0.265 (0.004)	0.293 (0.006)	0.381 (0.006)
$FWHM_{(622)}$ / °	0.283 (0.005)	0.275 (0.005)	0.262 (0.004)	0.291 (0.006)	0.379 (0.006)

Note: The errors were shown in the parentheses.

Table S3 Crystallite size and strain of Au doped samples (Size/Strain mode)

Sample	Au-1	Au-2	Au-3	Au-4	Au-5
Size	299 (6) Å	316 (4) Å	325 (5) Å	293 (5) Å	223 (8) Å
Strain	0.00%	0.00%	0.00%	0.00%	0.00%
R	1.0	1.0	1.0	1.0	1.0

Note: The errors were shown in the parentheses. In the *Strain Only* mode, the strains from Au-1 to Au-5 were 0.6551%, 0.6209&, 0.6011%, 0.6669% and 0.8732, respectively. And their errors were 0.01381%, 0.01201%, 0.01121%, 0.01528% and 0.00939%, respectively. It is obvious that the effect of strain on the peak shape can be ignored.

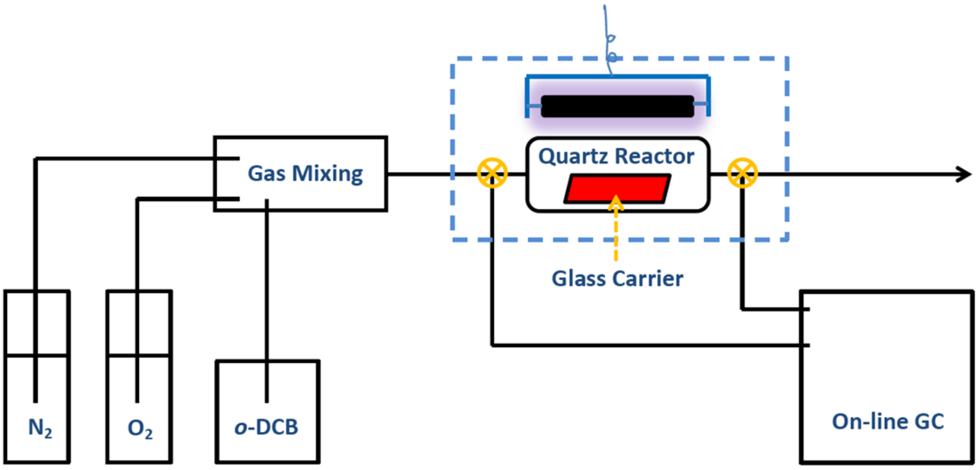

Fig. S1 Schematic diagram of the gas catalysis. Catalysts powders were loaded on the glass carrier, which was directly irradiated with a UV lamp. Temperature was controlled by a digital temperature controller in a heated fume hood (blue dotted area).

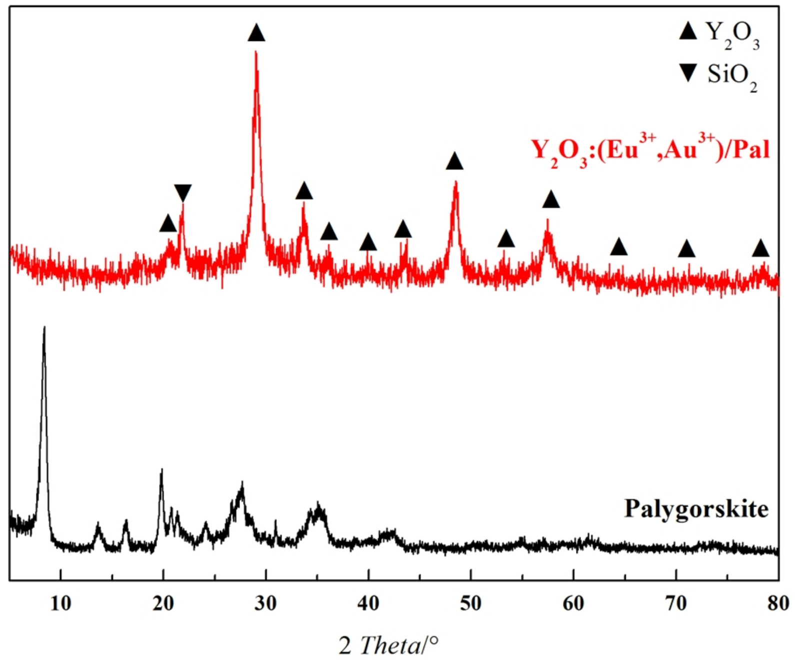

Fig. S2 Structure change of palygorskite. The characteristic reflection of Pal located at 8.3° disappeared and the reflection belonging to silicon oxide (PDF#29-0085) appeared, which means Pal has transformed to SiO_2.

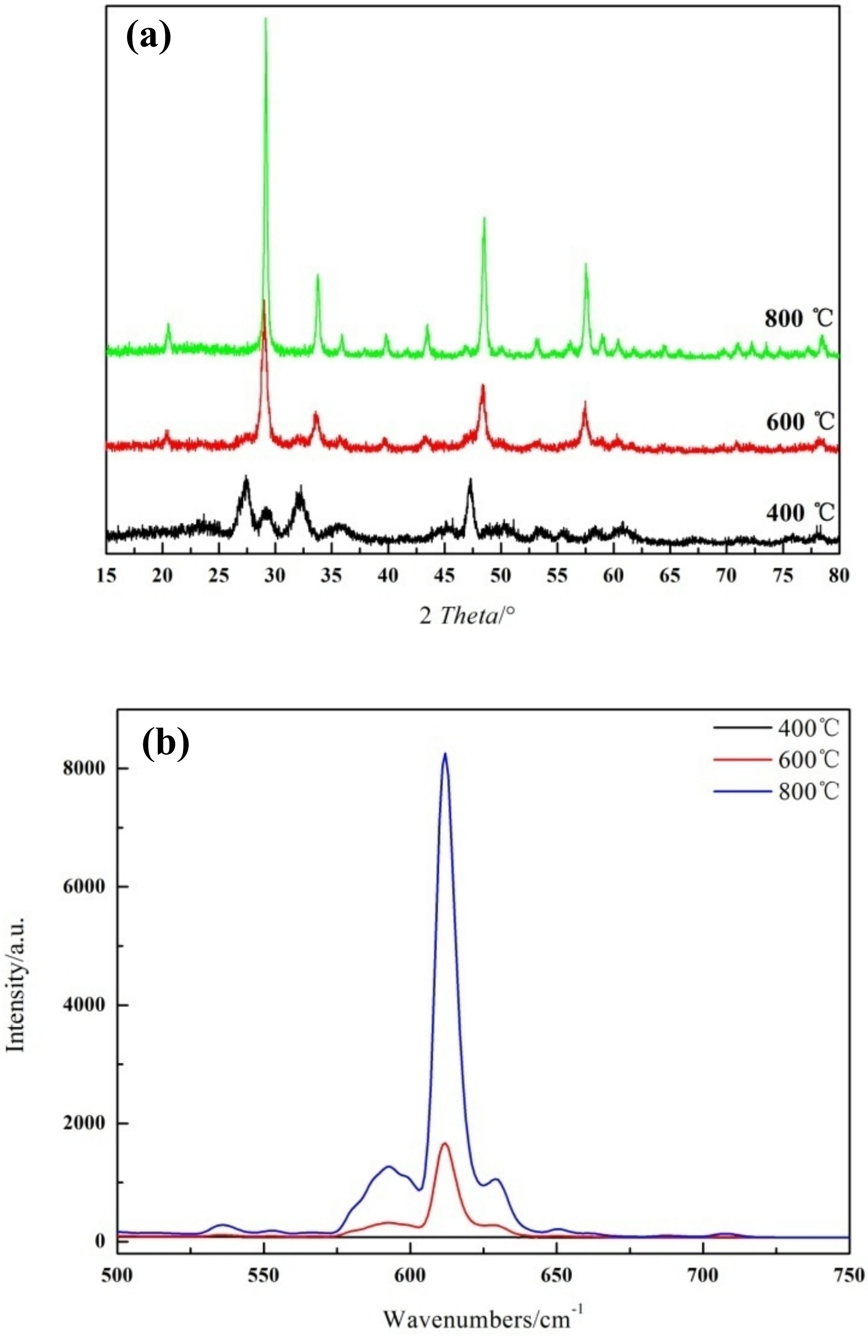

Fig. S3 (a) XRD patterns and (b) fluorescence spectra of the samples calcined at different temperatures. Sample calcined at 400 ºC showed no fluorescence property which was due to the lack of Y_2O_3 crystalline. Intensive red emission was observed in the sample calcined at 800 ºC, which showed a preferable crystallinity.

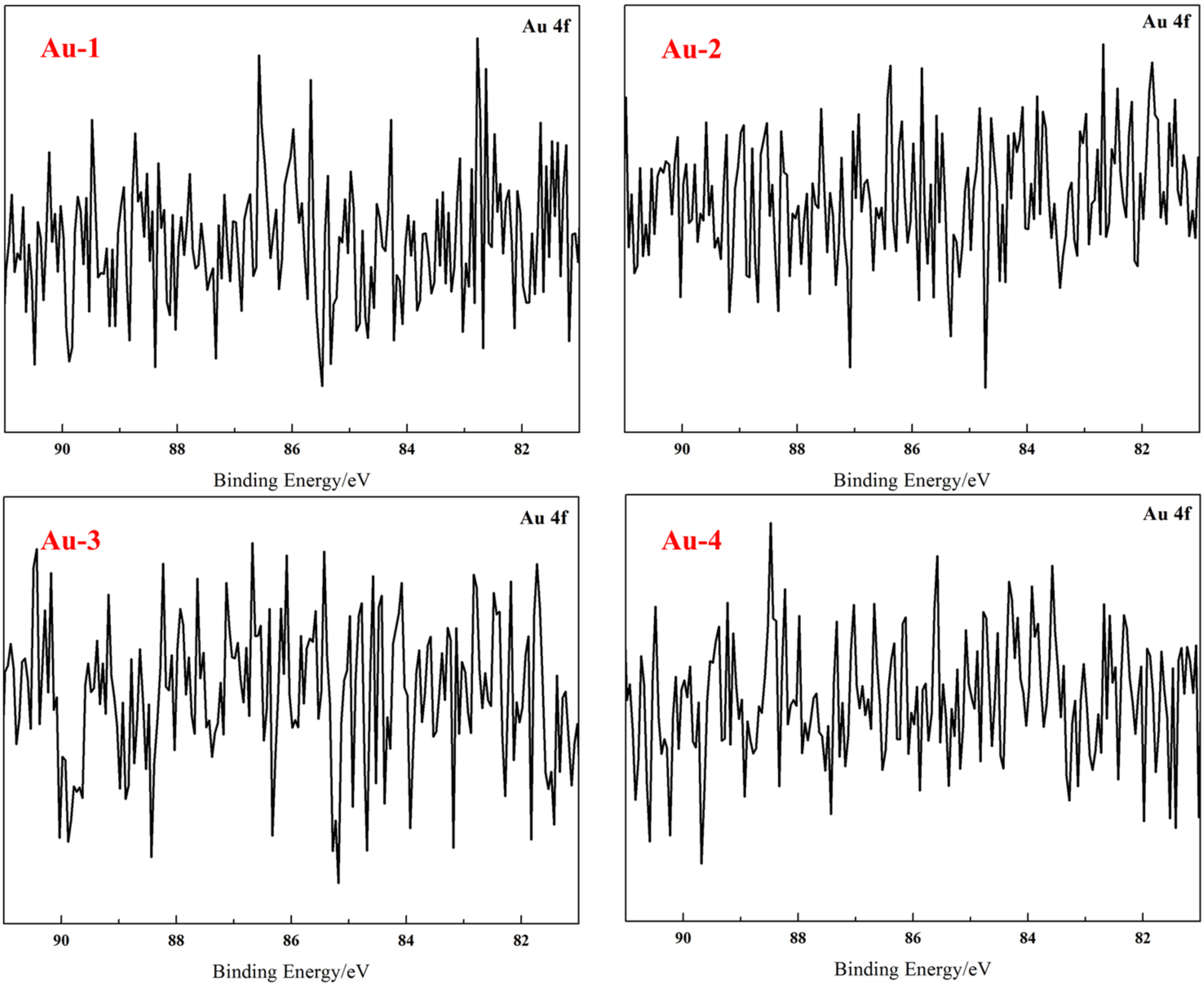

Fig. S4. Au 4f XPS spectra of other samples. Neither metallic Au nor Au^{3+} was observed.

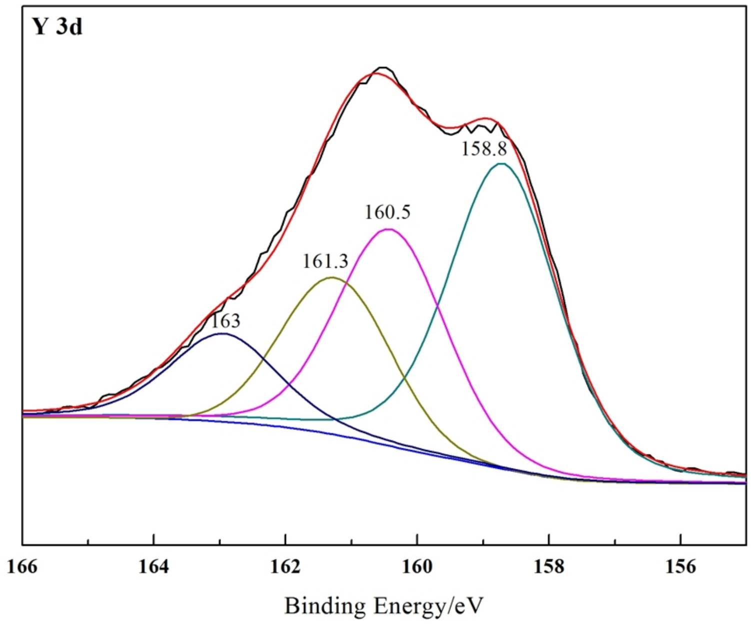

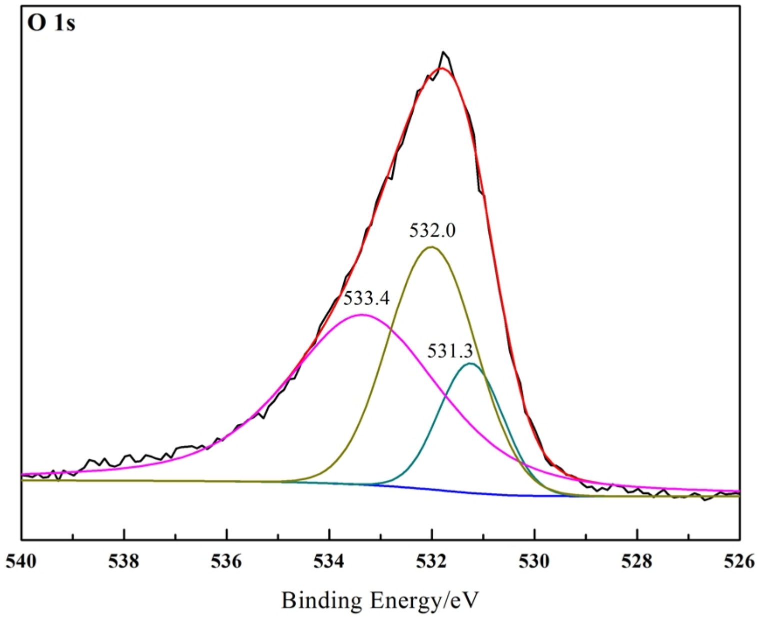

Fig. S5 XPS spectra of Y_2O_3:Eu^{3+}. Binding energy at 158.5 eV belonged to yttrium-hydroxyl bonding (doi:10.1016/S0368-2048(01)00312-7), which was from the hydrolysis of Y_2O_3. The higher binding energy at 160.5 eV was close to the value for pure YF_3 (doi:10.1021/cm980580n), which might be caused by the presence of hydrogen. Binding energies at 531.3 and 532.0 eV belonged to hydroxyl groups on the nanoparticle surface (doi:10.1016/S0368-2048(01)00312-7). Binding energy at 533.4 eV was from adsorbed water oxygen.

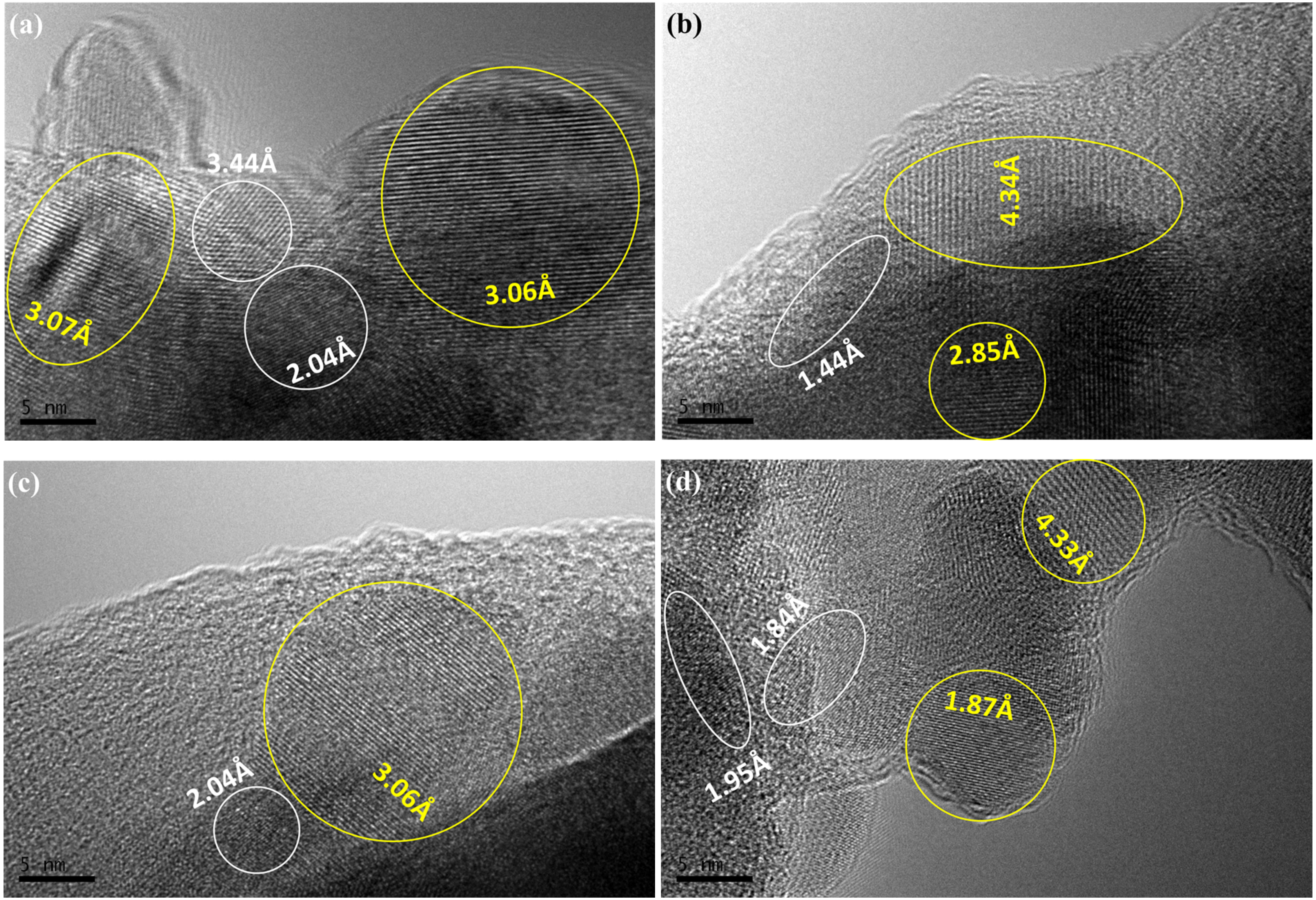

Fig. S6 HRTEM images of Au-5. The interplanar distances of 2.04 and 1.44Å coincided with planes (200) and (220) of metallic gold (PDF#04-0784), respectively. The interplanar distances of 3.44, 1.95 and 1.84 Å were attributed to planes (111), (620) and (202) of Au_2O_3 (PDF#43-1039), respectively. The interplanar distances of 4.34, 3.06, 2.85 and 1.87 Å were from planes (211), (222), (321) and (440) of Y_2O_3 (PDF#41-1105), respectively.

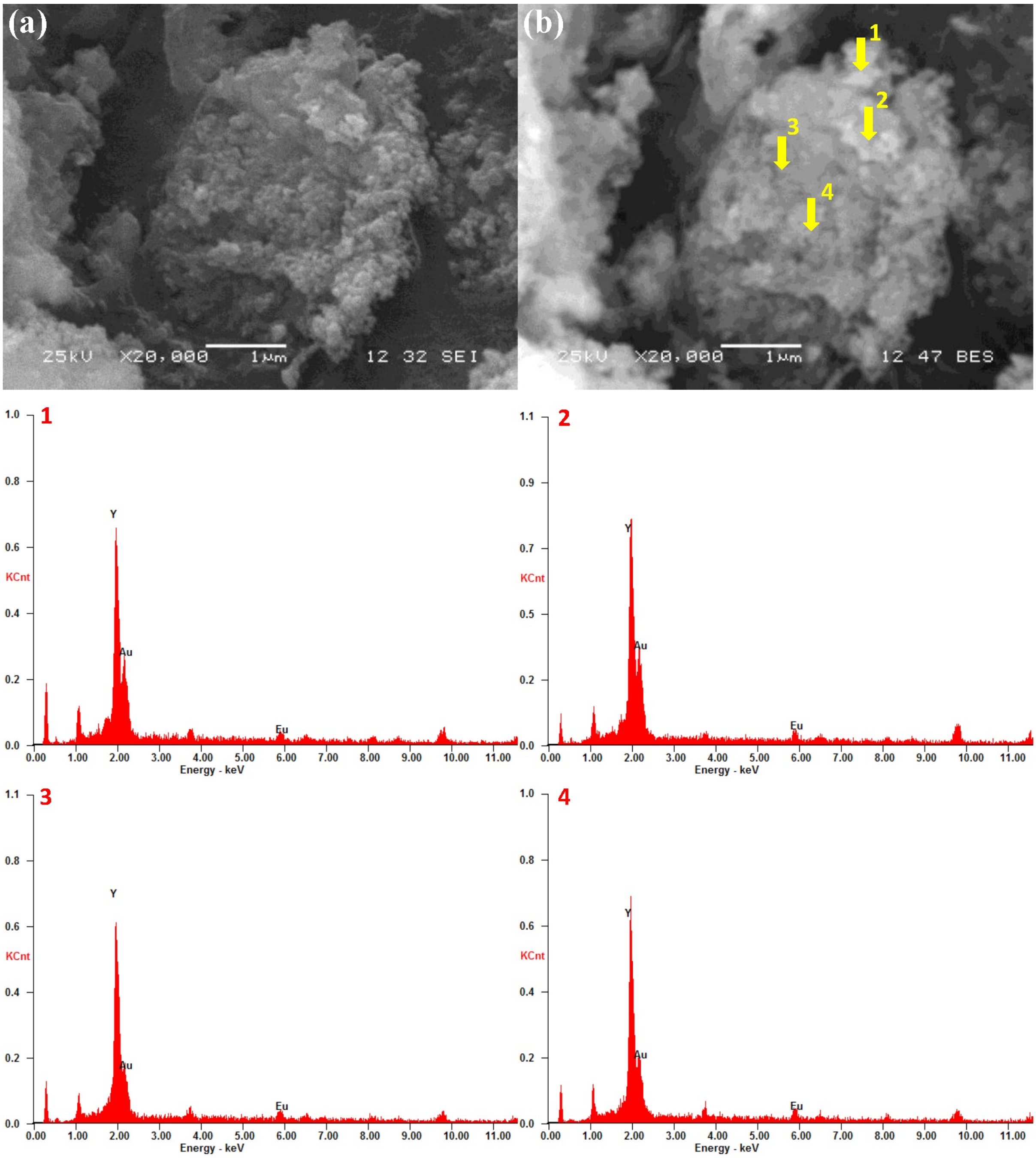

Fig. S7 (a) SEM and (b) BES images, and corresponding EDX spectra of Y_2O_3:(Eu^{3+},Au^{3+}) sample.

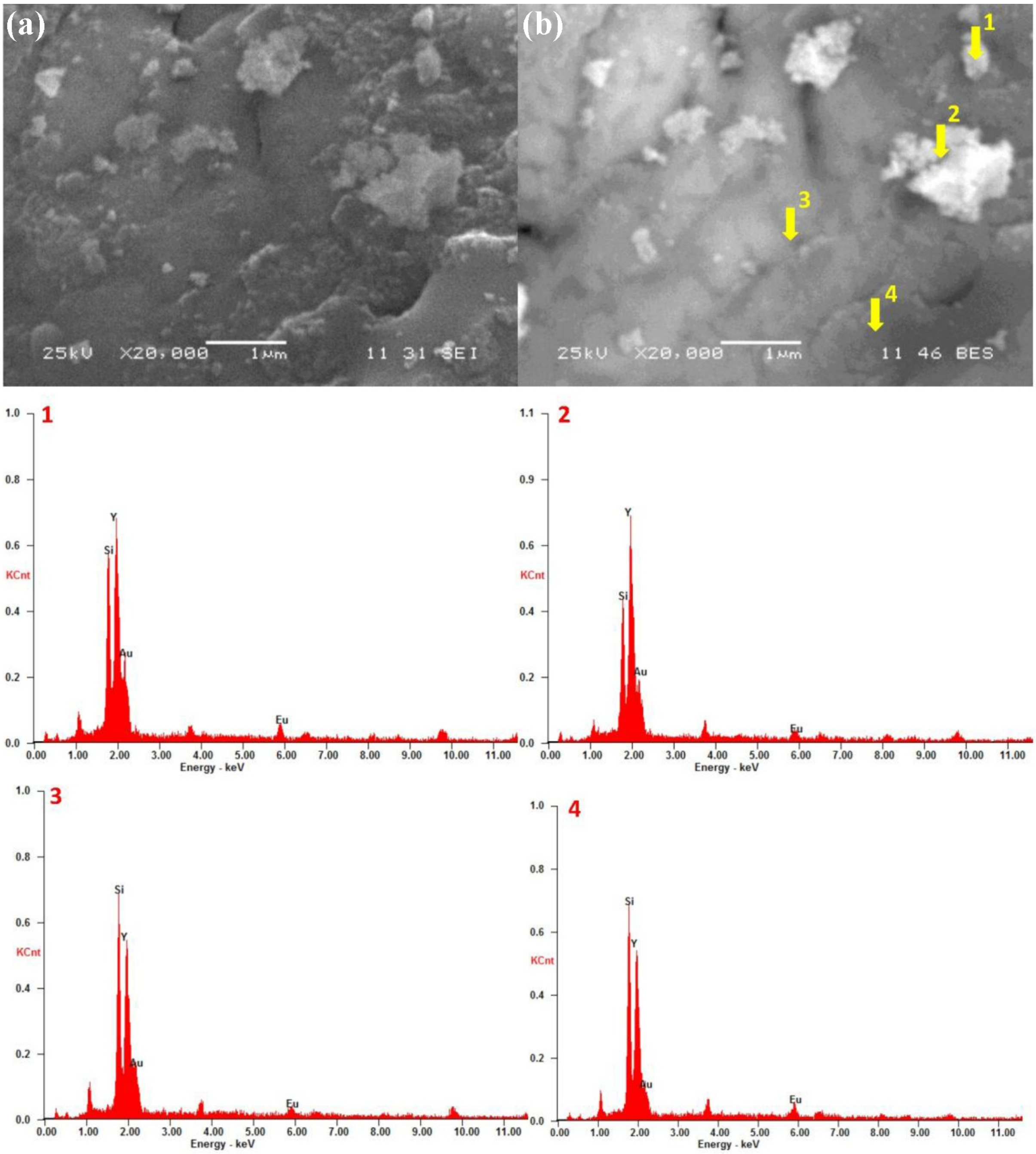

Fig. S8 (a) SEM and (b) BES images, and corresponding EDX spectra of Y_2O_3:(Eu^{3+},Au^{3+})/Pal.

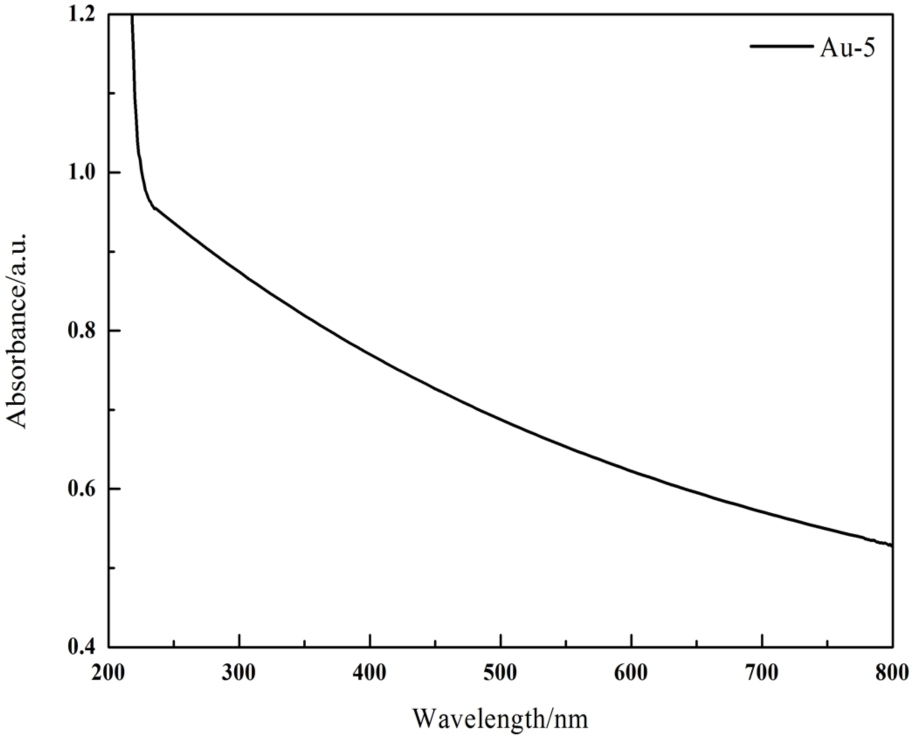

Fig. S9 UV-Vis absorption spectrum of Au-5. Absorption peak would reflect in the range of 300-800 nm (doi: 10.1021/ac0702084) if the surface plasmon resonances of Au was triggered. However, no obvious absorption was observed in this work.

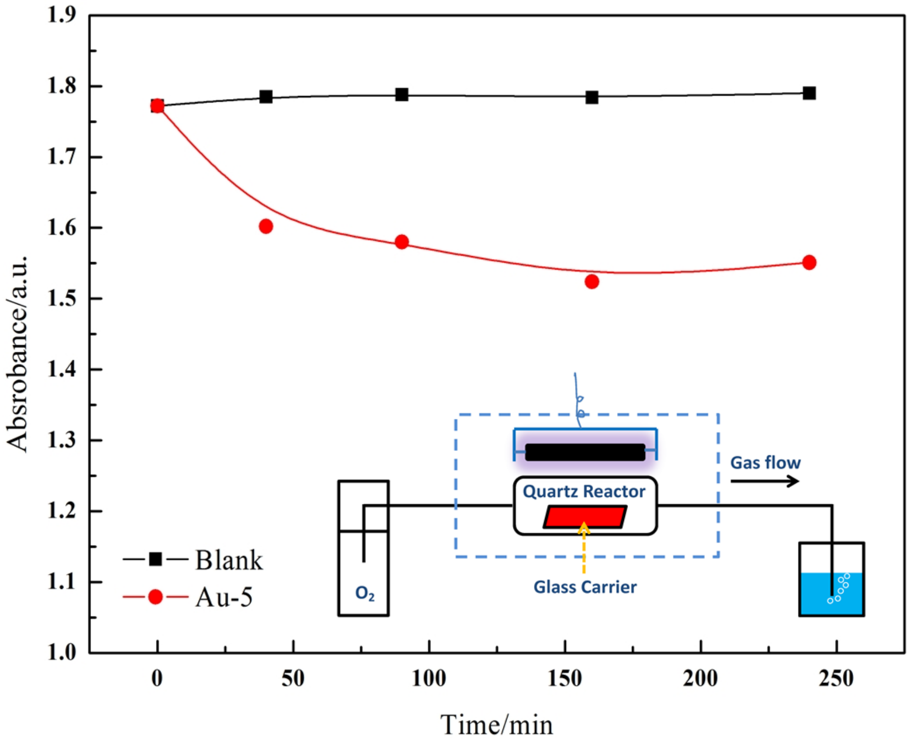

Fig. S10 Degradation of methylene blue was used to prove the formation of oxidant. O_2 flew through quartz reactor to the solution of methylene blue (MB), whose absorbance (maximum absorbance at 662 nm) would reduce when oxidant were produced. The blank experiment (without sample) was conducted under the same condition simultaneously. MB (100 mg/L) was kept in dark during the whole experiment, the temperature of MB solution was maintained at 25.0 ºC.

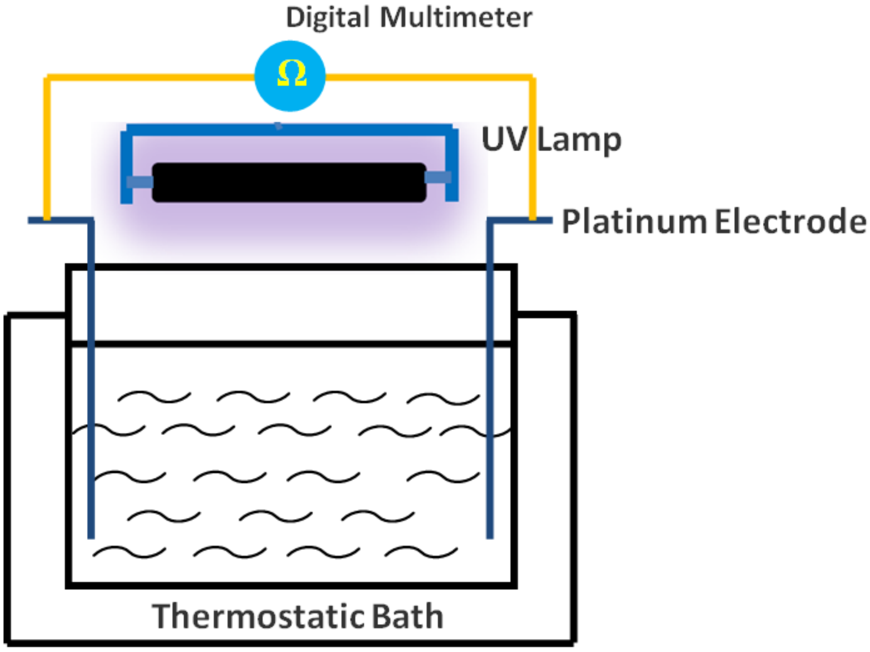

Fig. S11 Schematic diagram of the resistance analysis. The resistance analyzing was performed in a square quartz cell (Ø40 mm × 25 mm), which was kept in a thermostatic bath (25.0 ºC). Two platinum slices (5 mm × 15 mm) were used as electrodes. They were washed by hydrochloric acid, deionzed water and ethanol several times before analyzing. 20.0 ml deionzed water was used to disperse 30.0 mg Au-5 or Y_2O_3:Eu^{3+} powders respectively. Resistance of the mixture solution was analyzed before and after irradiation (254 nm) for 10 min. In the blank experiment, the resistance of 20.0 ml deionzed water increased from 328 KΩ to 422 KΩ, while that of Y_2O_3:Eu^{3+} and Au-5 mixture increased from 126 KΩ to 166 KΩ and 200 KΩ to 220 KΩ, respectively. Water can not be decomposed by radiation with wavelengths longer than 190 nm (doi:10.1038/238037a0). Another three facts that could affect the solution resistance were free ions, temperature and microorganism, respectively. Microorganism was the fact that affected the resistance as the temperature of deionzed water was maintained and microorganism was sensitive to UV irradiation. In other words, the elimination of the microorganism in deionzed water was the reason of resistance increasing. Y_2O_3 was sensitive to H_2O, and hydrolysis process happened at room temperature. OH- ions were produced in the hydrolysis process. Therefore, the initial resistance of Y_2O_3:Eu^{3+} mixture was lower than that of deionzed water. However, the initial resistance of Au-5 mixture was lower than deionzed water but higher than that of Y_2O_3:Eu^{3+}, which suggested that the hydrolysis of Y_2O_3 was partly prevented by surface Au. After irradiation, the resistance of Au-5 mixture increased 10% while others increased 28.6% and 31.7%, respectively. It is obvious that energy was transferred by metallic Au in Au-5, therefore the damage to the microorganism caused by UV irradiation was limited and the resistance was slightly increased.